Initial Evaluations of LoC Prediction Algorithms using the NASA Vertical Motion Simulator

Kalmanje Krishnakumar [*], Vahram Stepanyan [†], Jonathan Barlow [‡], Gordon Hardy [§], Greg Dorais [¶], Chaitanya Poolla [‖], Scott Reardon [**], and Donald Soloway [††]

NASA Ames Research Center, Moffett Field, CA 94035

Flying near the edge of the safe operating envelope is an inherently unsafe proposition. Edge of the envelope here implies that small changes or disturbances in system state or system dynamics can take the system out of the safe envelope in a short time and could result in loss-of-control events. This study evaluated approaches to predicting loss-of-control safety margins as the aircraft gets closer to the edge of the safe operating envelope. The goal of the approach is to provide the pilot aural, visual, and tactile cues focused on maintaining the pilot's control action within predicted loss-of-control boundaries. Our predictive architecture combines quantitative loss-of-control boundaries, an adaptive prediction method to estimate in real-time Markov model parameters and associated stability margins, and a real-time data-based predictive control margins estimation algorithm. The combined architecture is applied to a nonlinear transport class aircraft. Evaluations of various feedback cues using both test and commercial pilots in the NASA Ames Vertical Motion-base Simulator (VMS) were conducted in the summer of 2013. The paper presents results of this evaluation focused on effectiveness of these approaches and the cues in preventing the pilots from entering a loss-of-control event.

I. Introduction and Background

Loss-of-control (LoC) events are typically triggered when flying near the edge of the safe operating envelope due to uncertainties and non-linear nature unknown to the pilot. Edge of the envelope here implies that small changes or disturbances in system state or system dynamics can take the system out of the safe envelope in a short time and could result in catastrophic events. Figure 1 illustrates the concept of edge of the flight envelope as defined in this paper. Essentially at the edge, normal piloting actions (inputs) lead to abnormal flight (outputs) due to lack of robustness, unmanaged uncertainties, failures, etc.

LoC events have been the number one contributing factor to fatal airline accidents, and have resulted in more fatalities than any other factor during the past ten years (see for example Ref.[1]). Generally, LoC is characterized in Ref.[2] as motion that is:

- outside the normal operating flight envelopes
- not predictably altered by pilot control inputs
- characterized by nonlinear effects, such as kinematic/inertial coupling, disproportionately large responses to small state variable changes, or oscillatory/divergent behavior
- likely to result in high angular rates and displacements

[*]Tech Area Lead, Autonomous Systems and Robotics, Intelligent Systems Division, Associate Fellow AIAA, kalmanje.krishnakumar@nasa.gov

[†]Senior Scientist, UARC, University of California Santa Cruz, Senior Member AIAA, vahram.stepanyan@nasa.gov

[‡]Research Scientist, Stinger Ghaffarian Technologies Inc., Member AIAA, jonathan.s.barlow@nasa.gov

[§]Research Pilot, Science Application International Corp., Member AIAA, gordon.h.hardy@nasa.gov

[¶]Applied Avionics Software Group lead, Intelligent Systems Division, Member AIAA, gregory.dorais@nasa.gov

[‖]Research Engineer, Stinger Ghaffarian Technologies Inc., Member AIAA, chaitanya.poolla@nasa.gov

[**]Flight Simulations Engineer, Aviation Systems Division, Member AIAA, scott.reardon@nasa.gov

[††]Research Scientist, Intelligent Systems Division, Member AIAA, donald.i.soloway@nasa.gov

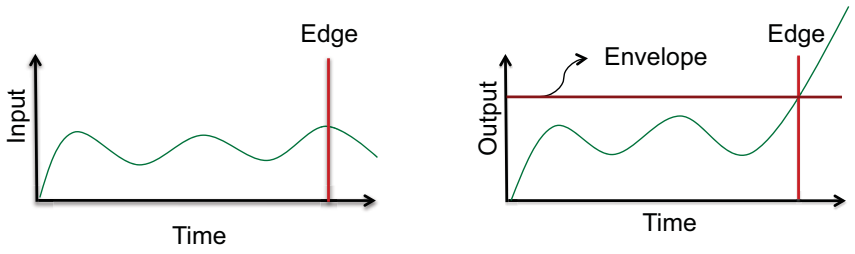

Figure 1. Conceptualization of flying on the edge.

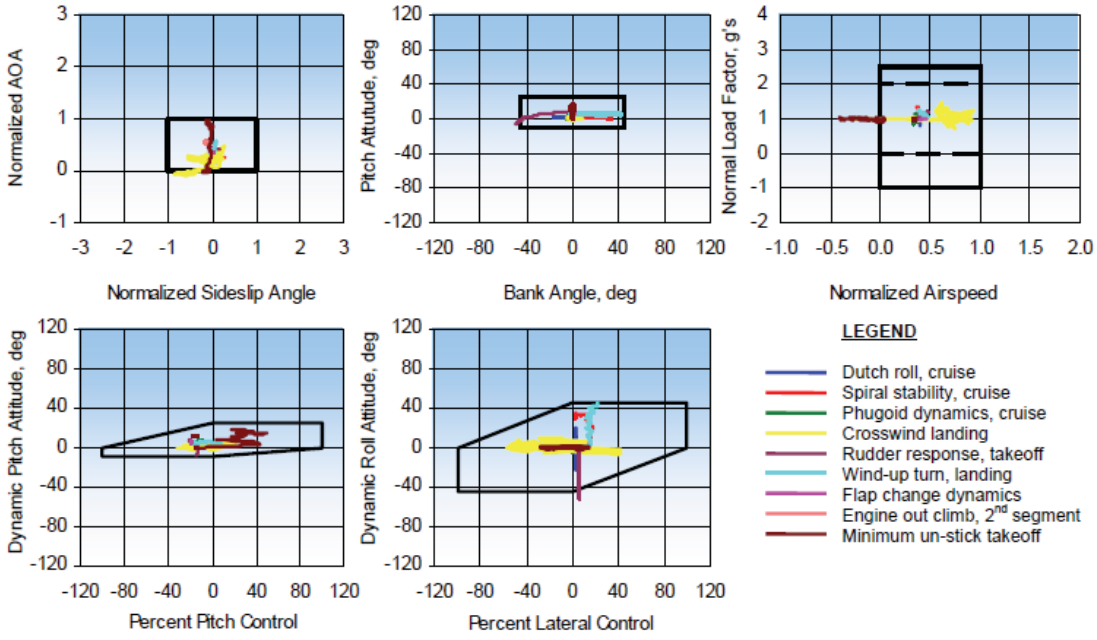

Figure 2. Quantitative LoC Criteria and flight data from Ref.[2]

- characterized by the inability to maintain heading, altitude, and wings-level flight.

Historically, LoC has been determined to be a factor in an accident by qualitative judgment based upon accident investigation experience. Quantitative LoC criteria (see Ref.[2] for details) have been created to define LoC events. These criteria are in the form of boundary boxes on combinations of system states and control inputs, as seen in Figure 2. These boundaries are based on a set of historical LoC events. The authors of Reference proposed that violation of any three of the quantitative LoC criteria constitutes LoC, violation of any two boundaries is borderline LoC, and typical aggressive flight test maneuvers typically violate at most one boundary. Our work evaluated in this paper combines multiple of the Quantitative LoC criteria into a single composite predictive boundary that aids the pilot in avoiding LoC scenarios. Particularly, the evaluation of the pilot feedback cues as detailed in Section D combines elements of the Pitch Attitude, Bank Angle, Dynamic Pitch Attitude, Dynamic Roll Attitude, Percent Pitch Control, and Percent Lateral Control criteria into a one two-dimensional display (discussed in Section D). Details of the algorithms evaluated can be found in an earlier paper referenced in Ref.[3]

In the rest of the paper, we discuss the following: (1) the cueing architecture; (2) simulation evaluation description; (3) VMS pilot-in-the-loop evaluation results and discussion; and (4) conclusions and recommendations based on this study.

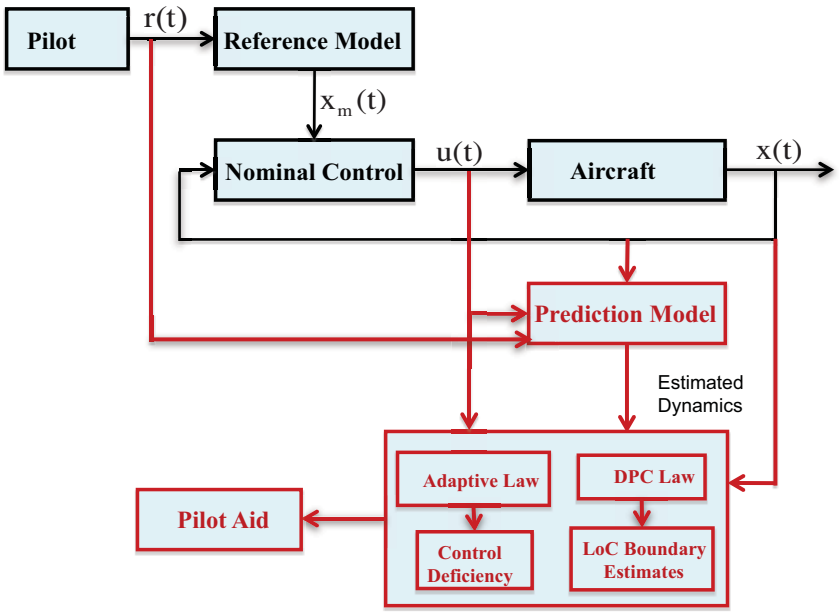

Figure 3. The Predictive Architecture.

II. LoC Cueing Architecture

The LoC detection and prevention technology is a plug-in type architecture that can work parallel to the on-board computing devices without interfering with the flight control system, the schematics of which is shown in Figure 3. The black boxes and signals form the baseline aircraft control architecture, and are unmodified for this work. The baseline flight control system represents the manufacturer's original design that meets all of the stability and performance requirements as mandated by the certification criteria. The predictive architecture includes the red boxes, which are the prediction model, the adaptive law, the control deficiency/stability margin estimates, the data based predictive control law (DBPC), the LoC boundary estimates, and the pilot aid. This architecture uses data available from the real time measurements, including pilot command $r(t)$, aircraft control signal $u(t)$, and available sensed aircraft state $x(t)$. The prediction model along with the adaptive law use the available data to produce estimated aircraft dynamics in the form of linear time varying system and the estimate of the control deficiency. The DBPC algorithm utilizes the pilot's inputs, aircraft state time histories recorded over a time window, and the estimated dynamics to produce the pilot's maneuverability margins in the form of two dimensional visual cue. The magnitude of the control deficiency estimate (CDE) is used to trigger the display of the box to the pilot, thus indicating the safe operational region in both longitudinal and lateral directions. In addition, there is a force feedback mechanism associated with the bounding box that can be applied to the pilot's stick to increase the stick resistance as it moves toward the box boundary. For more details of this aspect of the study, please see Reference.[4] For more details of the LOC Cueing architecture, including the theoretical analysis, please see References.[3,5–7]

III. Simulation Evaluation Description

A. Transport Class Aircraft Model (TCM)

For this simulation study, a generic, non-proprietary, twin-jet, under-the-wing, transport class aircraft model (TCM) was used, which was developed at NASA Langley Research Center (LaRC).[8] It is based on a 5.5% sub-scaled model of a twin-jet generic transport aircraft (GTM) developed at LaRC to collect wind tunnel aerodynamic data (see Refs.[9,10] for details).

These data were later modified to include potentially extreme attitudes (the angle of attack ranging from -5 to 85 degrees, and the sideslip angle ranging from -45 to 45 degrees) to address transport aircraft safety issues such as loss-of-control due to inadvertent stalls, environmental disturbances, or aircraft system

failures. The modifications also included appropriate scaling of the GTM dimensions to produce TCM values for wing span and surface area, wing chord length, CG location, and engine location. The TCM weight and moments of inertia were selected to be representative of a mid-weight, twin-jet transport aircraft. In addition, Reynolds number adjustments to the data were made to account for the air flow differences between the GTM and TCM.[8]

The engine model used for the TCM simulation was developed at Glenn Research Center (GRC) and is representative of a turbofan jet engine with a maximum sea-level thrust of approximately 40,000 lbs. It is modeled as a first-order system of the engine fan speed with a time constant depending on the altitude. It also includes time delays that vary as a function of fan speed, altitude, Mach number, and throttle command, and is subject to a variable rate limit.

The TCM surface actuator models representative of hydraulic actuators, which have response times and non-linear characteristics that are typical for full-scale transport aircraft, such as variable rate limiting and variable position blow-down limits.

The original TCM model was equipped with an auto-throttle control block, and a nonlinear dynamic inversion based proportional-integral attitude-hold flight control that was developed in-house for this simulation study.

The TCM damage models were approximated using a modified vortex-lattice code developed at the Ames Research Center.[11] Detailed geometric models of the aircraft were generated for various damage configurations, including losses of portions of the wing, horizontal tail, and vertical tail.[12] These geometric models were then used to generate estimates of the aircraft aerodynamic coefficients, stability derivatives and inertia data for the various damage models.

B. VMS Facility

The Vertical Motion Simulator (VMS) is the ideal facility to simulate LoC scenarios and to test the cueing technology's effectiveness because of the VMS's large motion envelope. The VMS motion system, shown in Figure 4, is an uncoupled, six-degree-of-freedom motion simulator. It is located in, and partially supported by, a specially constructed 120 ft tower.

The VMS is the ideal facility to simulate LoC scenarios and to test the cueing technology's effectiveness because of the VMS's large motion envelope. The VMS motion system, shown in Figure 4, is an uncoupled, six-degree-of-freedom motion simulator. The VMS system motion capabilities are provided in Figure 5. Included in the table are two sets of limits: system limits that represent the absolute maximum levels of attainable under controlled conditions; and operational limits that represent attainable levels for normal piloted operations.

The cab, shown in Figure 6, serves as the aircraft cockpit. The evaluation pilot occupied the right seat, with an optional test engineer in the left. A computer image generation system creates the out-the-window visual scene for the six-window collimated display with the head-up display superimposed on the center window. Additional aircraft information was provided on three head-down displays at both pilot stations.

C. LoC Scenarios

We consider two failure scenarios leading to TCM loss-of-control. First is the abrupt change in stability and control derivatives as the aircraft flies at 1500 ft altitude with calibrated airspeed of 175 kts. This change was generated by the 25% loss of left wing tip and 100% loss of left aileron effectiveness. The failure was randomly introduced during a 30 sec period starting after a minute of flight with the nominal TCM. Neither the failure parameters nor the failure time was available to the TCM flight control system. Second failure scenario is the gradual change of the aerodynamics of TCM over a 10 sec time period starting at 80 sec flight of the nominal TCM. This change mimics asymmetric wing icing, when one of the wings has an excess drag and reduced lift, which also create additional yawing and rolling moments respectively. The resulting model has reduced stability margins in pitch and roll axes. In addition, pitch-yaw coupling effect is generated, when the aircraft is banked to the affected wing.

D. Cueing Technologies

Aural, visual and tactile cues were given to the pilot. The aural cue was an alert triggered once per test run by the control deficiency estimate (CDE) crossing a predetermined threshold (see Figure 7). Once the alert was

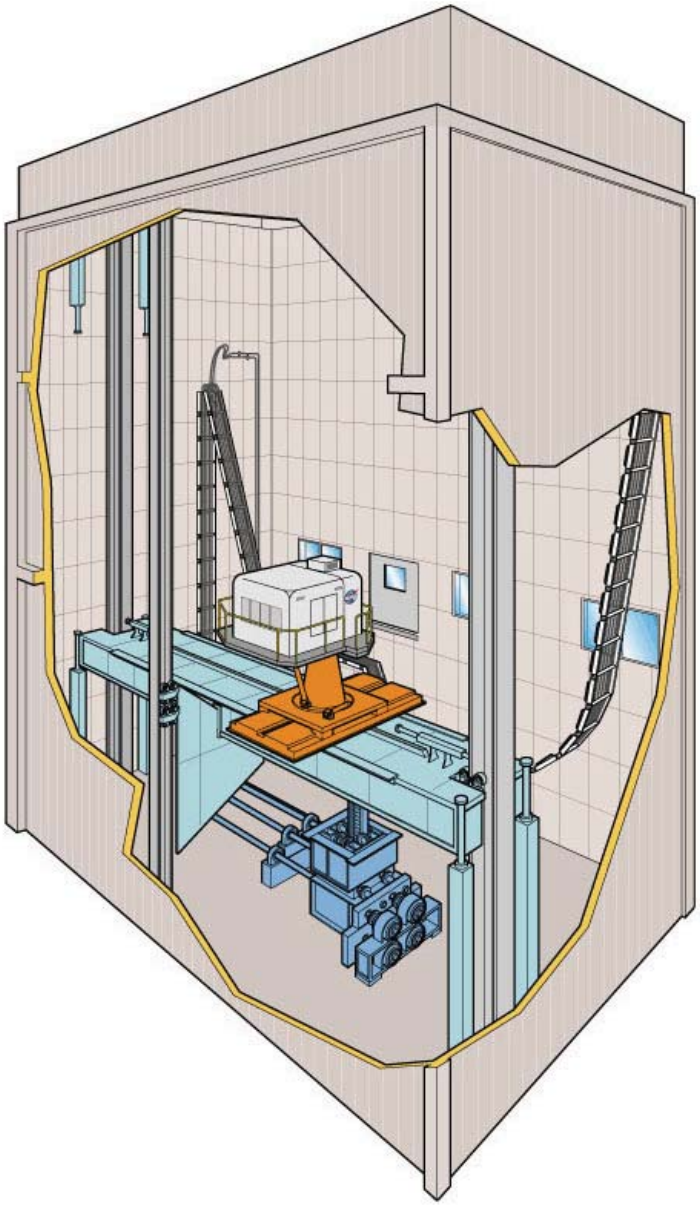

Figure 4. VMS facility.

triggered, it sounded continuously until canceled by the pilot. The visual cue was a dynamic stick position indicator and a dynamic loss-of-control boundary, which were overlaid on the heads-up display (HUD) (see Figure 8). The boundary was calculated by the data-based predictive control margins estimation algorithm. For this experiment, color was used to distinguish the loss-of-control visual cues from the baseline HUD, however further work is needed to determine appropriate symbols and placement for cueing with mono-color HUD and cockpit displays. The tactile cue was a force applied through the flight controls. The high-fidelity flight controls are heavily modified and optimized McFadden hydraulic force-loader systems, and a custom digital-control interface allows for comprehensive adjustment of the controller's static and dynamic characteristics. The tactile cue was calculated by the STI force-cueing algorithm (see Ref.[4] for details), and applied as an additive force, while leaving the baseline force curves unmodified.

Degree of Freedom	Displacement		Velocity		Acceleration	
	System Limits	Operational Limits	System Limits	Operational Limits	System Limits	Operational Limits
Longitudinal	± 4 ft	± 4 ft	± 5 ft/sec	± 4 ft/sec	± 16 ft/sec^2	± 10 ft/sec^2
Lateral	± 20 ft	± 15 ft	± 8 ft/sec	± 8 ft/sec	± 13 ft/sec^2	± 13 ft/sec^2
Vertical	± 30 ft	± 22 ft	± 16 ft/sec	± 15 ft/sec	± 22 ft/sec^2	± 22 ft/sec^2
Roll	± 0.31 rad	± 0.24 rad	± 0.9 rad/sec	± 0.7 rad/sec	± 4 rad/sec^2	± 2 rad/sec^2
Pitch	± 0.31 rad	± 0.24 rad	± 0.9 rad/sec	± 0.7 rad/sec	± 4 rad/sec^2	± 2 rad/sec^2
Yaw	± 0.42 rad	± 0.24 rad	±0.9 rad/sec	± 0.8 rad/sec	± 4 rad/sec^2	± 2 rad/sec^2

Figure 5. Table of VMS Motion System Performance Limits.

Figure 6. VMS Cab.

E. Simulation Tasks

The tasks for this study were based on standard approaches to SFO, which were slightly different for the two failure scenarios. For the first LoC scenario, the task was a left hand approach pattern beginning at 1500 ft with a heading of 55 deg and a velocity of 175kts. The approach was directed by a prerecorded air traffic controller's audio heading command, the details of which are illustrated in Figure 9. For the second scenario the task was a right hand approach pattern with an initial heading of 145 deg or a left hand approach pattern with an initial heading of 35 deg both at the altitude of 5000 ft and velocity of 200 kts, depending on which wing has been affected by the simulated icing condition. In both cases the approach was directed by the prerecorded heading command. The right pattern with the detailed heading commands are illustrated in Figure 10 with the left pattern being the mirror image of it. For both tasks the voice command was synchronized with the task at hand.

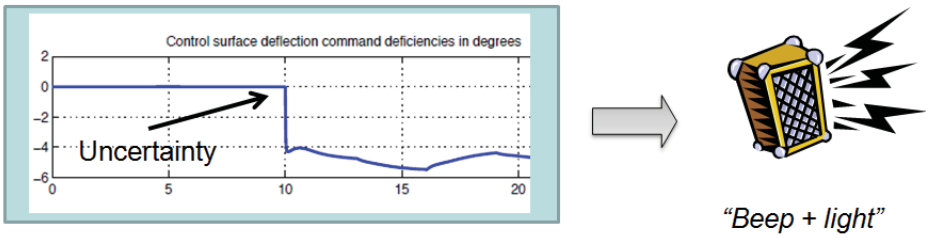

Figure 7. Aural cue.

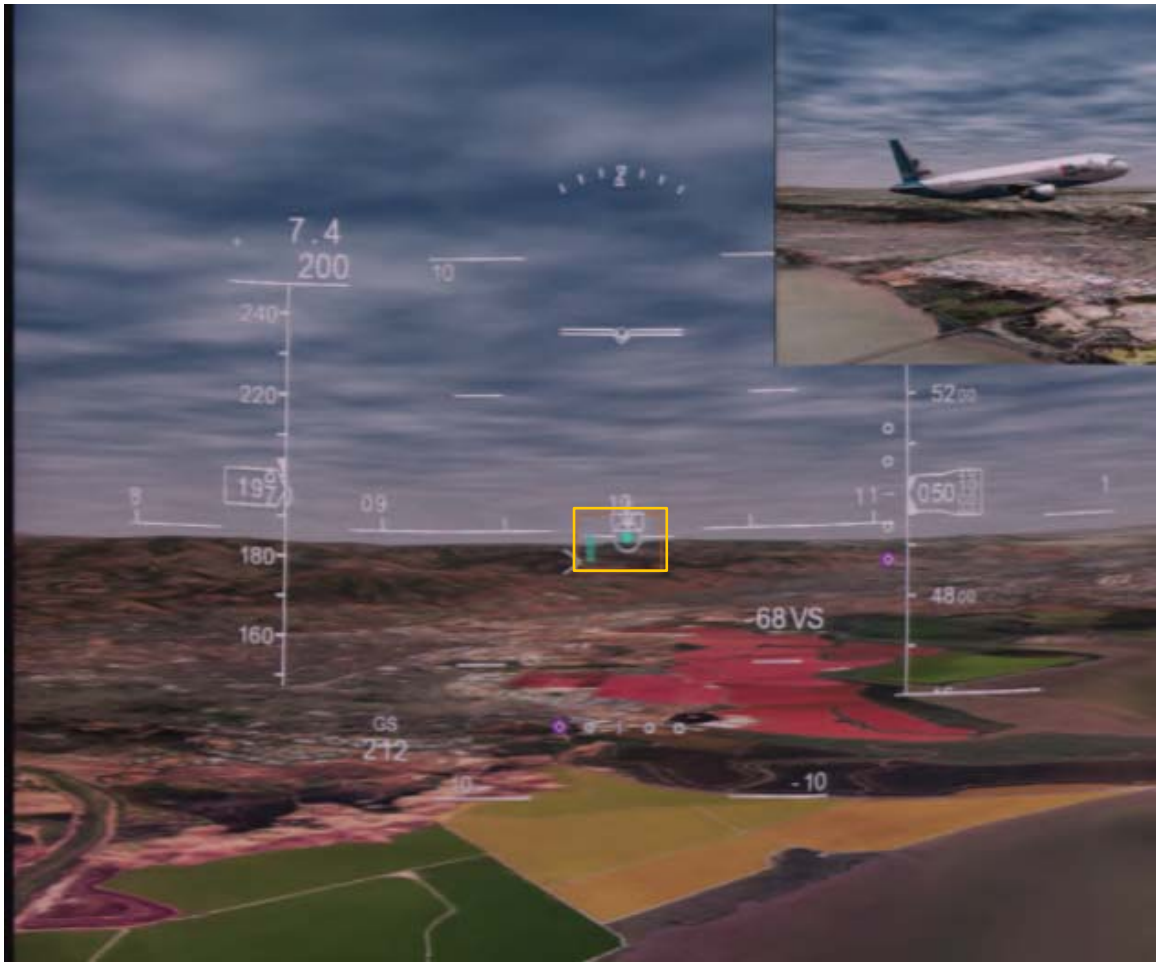

Figure 8. Visual cue.

F. Experimental Procedure

Pilots were presented with the technologies in five combinations: no cues, aural cue only, aural cue with visual cue, aural cue with visual and tactile cue together, and aural cue with tactile cue. The tactile and visual cues were never presented to the pilot without the aural cue.

The tasks and failures were presented to the pilot in a pseudo-random order, while making sure that the pilot has seen each combination of task, failure and technology at least twice. The tasks were further grouped by technology combination so that all scenarios for a given technology combination were given together, after

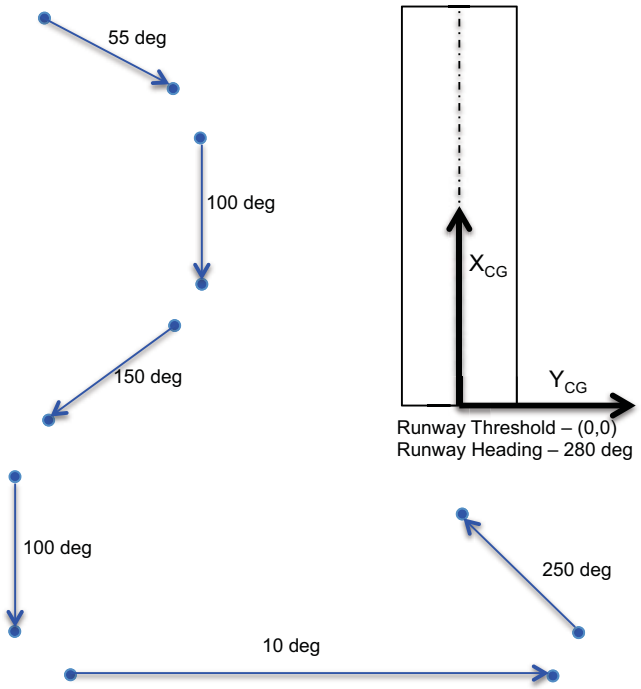

Figure 9. Simulation task for failure 1.

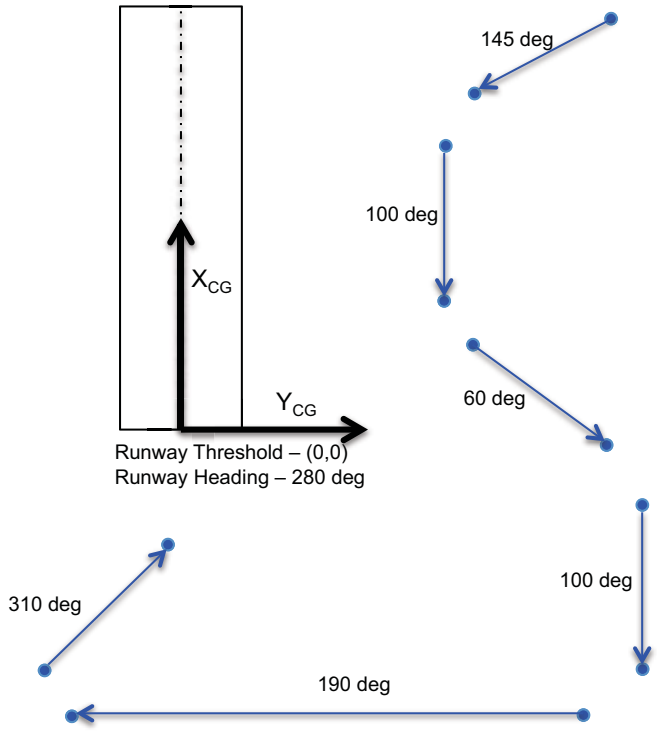

Figure 10. Simulation task for failure 2.

which the pilot was asked to fill out a questionnaire and provide comments. The technology combinations were also presented to the pilots in order of increasing complexity, beginning with no cues, followed by aural cue only, aural cue with visual cue, aural cue with visual and tactile cue together, and aural cue with tactile

cue, in that order. This was done to decrease the learning curve for the more complex technologies, as well as to help the pilot correctly interpret the tactile cue.

Each pilot was in the cockpit for 1 to 1.5 hours at a time, then out of the cockpit for the same amount of time while a second pilot was rotated in for testing. The use of two pilots allowed increased use of the VMS without overburdening the pilot.

G. Collection of objective and subjective Data

Both objective and subjective data were gathered during and between runs. Objective data were collected digitally and stored on a hard drive for non-volatile storage. At the beginning of each run in the form of all setup parameters for the cueing technologies and aircraft model, as well as initial aircraft states and trim values. During the runs, all model and cueing technology outputs were collected at 100 hz and screen captures were made of the in-cockpit attitude indicator and the out-the-window view. Subjective data was collected during the runs via video and audio recording of the pilot inside the cockpit during flight. After each set of runs, the pilots were asked to fill out a questionnaire and provide any additional comments, and the audio and video recording were continued to capture any verbal comments. Finally, after all tests were complete, each pilot was debriefed for overall comments and feedback.

IV. Evaluation Results and Discussion

A. Subjective Evaluation Summary

For the subjective evaluation, each pilot was asked to respond to a questionnaire with enough room for extra comments. The questionnaires for the aural and visual cues are presented in Figures 11 and 12.

LOC Warning Tone

	Strongly Disagree	Disagree	Neither Agree Nor Disagree	Agree	Strongly Agree
In the presence of a potential LOC scenario, the LOC Warning Tone aided my ability to retain control of the aircraft;	○	○	○	○	○
In the presence of a potential LOC scenario, the LOC Warning Tone aided my ability to safely complete the task;	○	○	○	○	○
The benefits of the LOC Warning Tone were clearly demonstrated when compared to the no guidance case.	○	○	○	○	○

Other Comments:

Figure 11. Pilot Feedback Questionnaire for the warning tone aural cue.

The comments received were very positive. Some of these are:

- "Once I was accustomed to the box it helped significantly."
- "Excellent tool to know the parameters ?"
- "As an a/c damage cue, it is very helpful."
- "I was mesmerized by the box and I dropped the other parts of the instrument check."
- "The bounding box significantly reduces the training curve. "

LOC Bounding Box Display

	Strongly Disagree	Disagree	Neither Agree Nor Disagree	Agree	Strongly Agree
In the presence of a potential LOC scenario, the LOC Bounding Box Display aided my ability to retain control of the aircraft;	○	○	○	○	○
In the presence of a potential LOC scenario, the LOC Bounding Box Display aided my ability to safely complete the task;	○	○	○	○	○
The benefits of the LOC Bounding Box Display were better when compared to the LOC Warning Tone case.	○	○	○	○	○
The benefits of the LOC Bounding Box Display were clearly demonstrated when compared to the No Guidance case.	○	○	○	○	○

Other Comments:

Figure 12. Pilot Feedback Questionnaire for the bounding box visual cue.

Overall, the pilots perceived the warning tone alone not to be very useful. The ratings for the bounding box visual cue were overwhelmingly positive as shown in Table 1.

Table 1. Pilot Scoring: 0 (Strongly Disagree) - 4 (Strongly Agree)

Pilot	A	B	C	D	E	F	G	H	J
Visual	3	4	4	3	3	4	4	4	4

B. Objective Evaluation

1. Quantitative Validation of Aural Cue Algorithm

One of the objectives of this study was the validation of the detection capabilities of CDE. For this purpose we analyze the test results with respect to three criteria:

1) False alarm - when the magnitude of CDE exceeds the preset threshold for the nominal aircraft.

There were a total of 31 runs with the nominal aircraft. CDE was computed as a three dimensional signal representing the deficiency in aileron, elevator and rudder deflection commands to the corresponding actuators in degrees. Its magnitude was recorded and compared to the threshold of 1.5 *deg* for each of these runs. The audio warning signal was associated with this threshold. In 25 cases, CDE magnitude was below the threshold, and no warning was triggered, indicating that the aircraft is functioning as it supposed to. In 6 cases, there was a false alarm, that is the audio warning went off, implying that CDE magnitude was exceeding the threshold. The analysis of the pilot's input and the aircraft's state shows that in all these cases the aircraft was at an unusual bank angle exceeding the normal envelope, or the pilot's lateral input rate was too high for the actuator's bandwidth. The representative time histories of CDE magnitude, bank angle, roll rate and the pilot's lateral stick command are displayed in Figures 13 and 14. It can be observed from the Figure 13 that the peak value of CDE at time 304 *sec* corresponds to the bank angle's peak value of 51 *deg*, which exceeds the nominal bank angle envelop of 45 *deg*. On the other hand, Figure 14

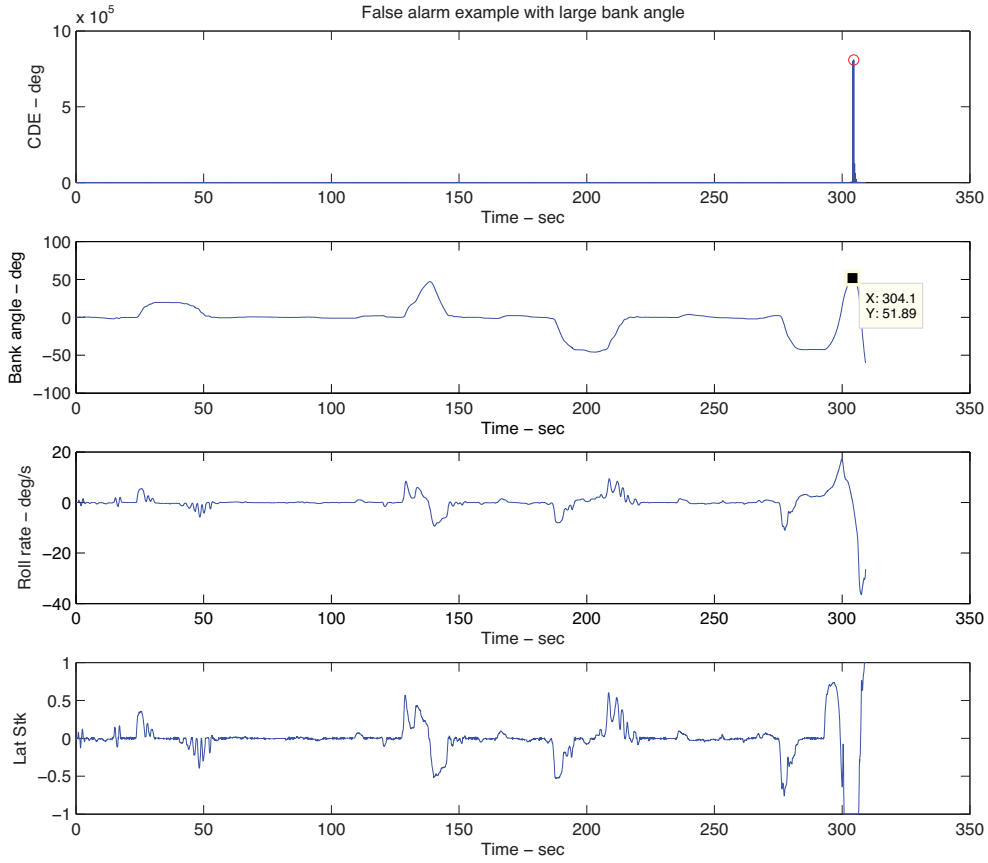

Figure 13. Control deficiency estimate, bank angle, roll rate and pilot's lateral stick command time histories in the case of false alarm associated with the large bank angle.

shows that the lateral stick's high rate at 62 *sec* generates the large value for CDE, thus triggering the alarm.

2) Missed alarm - when the magnitude of CDE stays below the preset threshold in the failure case.

There were total of 145 runs for the first failure scenario, and in all cases CDE exceeded the preset threshold, thus indicating that the aircraft is off nominal.

For the second failure scenario, there were a total of 175 runs. In all but two cases, the aircraft had crashed before the failure were introduced, CDE magnitude bound was higher than the threshold thus sending a right signal to the audio warning console.

3) Failure detection time lag - the difference between the audio alarm start time and failure start time.

We separately analyze the detection time for the first and second failure scenarios due to differences in the way they are introduced.

In the case of the first failure scenario, when the start time was randomized over a 30 *sec* window, CDE almost immediately jumped over the threshold in all 145 runs. The average detection lag time was 0.3 *sec* withe variance of 0.009 *sec*. The distribution of the time lag vs run number index is presented in Figure 15. This implies that the prediction algorithm was promptly triggered in the first failure case.

In the case of second failure scenario, the dynamics of the aircraft was changing gradually over a 10 *sec* time window, which causes CDE magnitude to change gradually from zero. Therefore the resulting detection time is larger than in the first case and averages to about 8 *sec* with the variance of about 1.5 *sec*. The distribution of the detection time lag is displayed in Figure 16. It can also be observed that for almost all runs the failure was detected before it was completely built up at 90 *sec*.

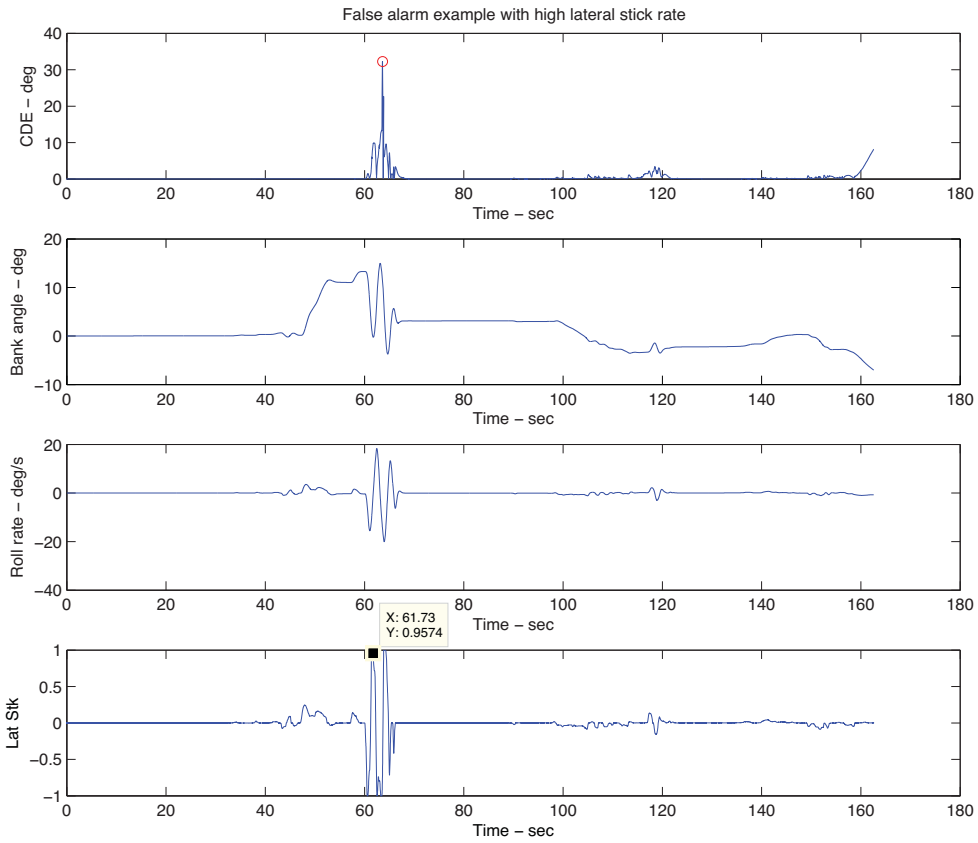

Figure 14. Control deficiency estimate, bank angle, roll rate and pilot's lateral stick command time histories in the case of false alarm associated with the high stick rate.

From this part of analysis we conclude that CDE performed well as a failure detection signal and as a trigger to LoC prevention algorithm.

2. Quantitative Validation of Visual Cue Algorithm

We examined two aspects in regards to validation of the algorithm: (1) Effectiveness of the visual cue in preventing LoC incidents; (2) Influence of pilot aggressiveness to the prediction algorithm.

Visual Cue Effectiveness

We present in Table 2 an analysis of time history data for the visual cue effectiveness. Four possible cases are explored for approximately 1.6 million time history data points recorded during the simulation study. The analysis examined for every time stamp if the pilot control activity was inside or outside the cue followed by examining the aircraft states after 4 seconds (prediction window) to record if the states were inside or outside of the LoC boundaries defined in Section I. Of the four cases shown in Table 2, Cases 1 and 2 show the effectiveness of the cue in preventing an unsafe situation. With a very high Case 1 percentage, it is clear that the cue was consistent with the expectation. The non zero Case 2 percentage is an undesirable result, and based on pilot feedback, it was determined that this was mainly caused by the algorithms inability to handle aggressive pilot actions. In the next subsection, we analyze the reasons behind this phenomenon.

Cases 3 and 4 document percentage of cases in which pilot control was outside of the cue. As expected, some of the flights exited the LoC boundaries (Case 3) and some did not (Case 4).

Influence of Pilot Aggressiveness

We used a simple measure of pilot aggressiveness. After the uncertainty is introduced, we measure the

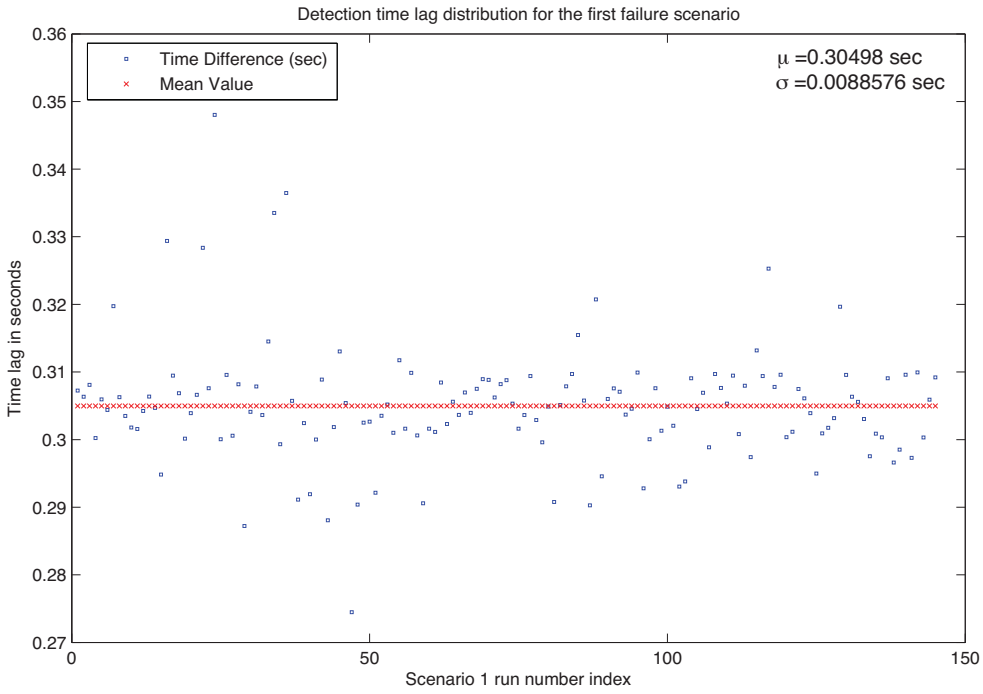

Figure 15. Detection time lag distribution with the mean and variance for the first failure scenario.

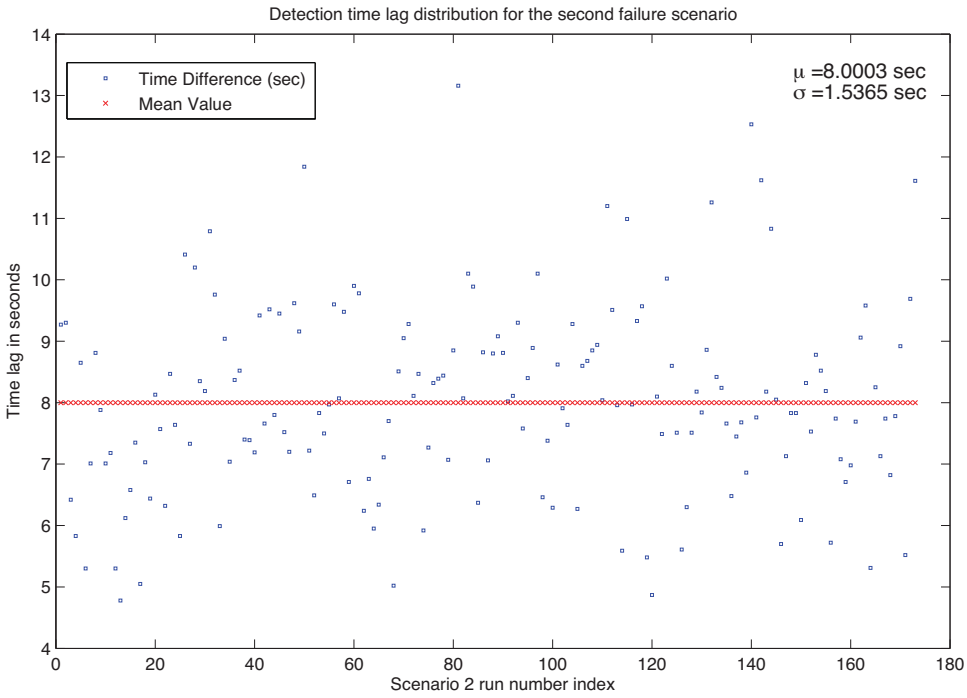

Figure 16. Detection time lag distribution with the mean and variance for the second failure scenario.

Table 2. Visual Cue Effectiveness Analysis.

Cases	Control activity inside the cue	LoC Boundaries violated (after 4*sec*)	% of flight data
1	YES	NO	93.8 %
2	YES	YES	3.3 %
3	NO	NO	1.7 %
4	NO	YES	1.2 %

rate of change of stick position as an indication of pilot aggressiveness. Using a threshold value for pilot aggressiveness (rate = 1 stick unit/sec), we examine the magnitude of CDE as computed by the algorithm. This magnitude is an indication of the inability of the aircraft to provide the requested control activity. We choose a threshold of 4.5 *degrees* for CDE for this analysis based on data for when the stick rate is less than 1 (see Table 3). If the algorithm is consistent with expectations, higher stick rate should lead to higher control deficiency for cases in which the aircraft violates the LoC boundaries leading to a total loss of the aircraft. This is illustrated in Table 3. For flights within the LoC boundaries (Safe flight), this correlation does not exist.

Table 3. Influence of the pilot aggressiveness

	Safe flight		Loss of aircraft	
	$CDE < 4.5$	$CDE > 4.5$	$CDE < 4.5$	$CDE > 4.5$
Stick rate < 1.0	99%	1 %	95%	5%
Stick rate > 1.0	42%	58 %	28%	72%

Based on the analysis presented above, it is concluded that Case 2 in the previous section was mainly caused by pilot's demand not being met by the aircraft's available control as perceived by the prediction algorithm. A big factor for this erroneous signal is the assumption in the prediction algorithm of near constant pilot control input (small stick rate) for the next 4 seconds. Future designs of this algorithm will consider this effect and adjustments to the prediction performance measure will be considered.

V. Conclusion

In this work, we have shown that usable controllability margins can be computed in real-time using predictive technologies and used as feedback cues to the pilot. Using ten pilots with varying experiences we have documented the efficacy of using simple cues to help prevent LoC incidents. This simulation study was conducted using the NASA Ames Vertical Motion Simulation facility. Our next step is to improve on the algorithm to better accommodate pilot aggressiveness in our predictive capabilities and evaluate these technologies using commercial airline pilots.

VI. Acknowledgments

This research was accomplished with the contributions of many individuals and organizations. The authors thank the pilots who participated in and provided insight during the preliminary and final simulation evaluations, including Gordon Hardy from NASA Ames Research Center, Manny Antimisiaris, Barton Henwood, Denis Steele, and Martin Trout from NASA Dryden Flight Research Center, Hal Cunningham, Phil Gallagher, Dave Perkins, and Phil Pullen from Flight Research Associates, and Mietek Steglinski from SGT, Inc. The authors are also thankful for the exceptional service and assistance provided by the NASA Ames Research Center VMS team. Finally, the authors extend their appreciation to the Vehicle Safety Systems Technologies (VSST) project within the NASA Aeronautics Research Mission Directorate for their support of this research.

References

[1]Statistical Summary of Commercial Jet Airplane Accidents Worldwide Operations 1959-2009, p. 23, Aviation Safety, Boeing Commercial Airplanes, Seattle, WA, USA, 2010.

[2]J. E. Wilborn and J. V. Foster, Defining Commercial Transport Loss-of-Control: A Quantitative Approach, Proceedings of the AIAA Flight Mechanics Conference and Exhibit, Providence, RI, August 2004.

[3]K. Krishnakumar, V. Stepanyan and J. Barlow , Piloting on the Edge: Approaches to Real-Time Margin Estimation and Flight Control, In Proceedings of the AIAA Guidance, Navigation and Control Conference, Minneapolis, MN, August 2011.

[4]D. H. Klyde, A. K. Lampton, D. J. Alvarez, N. D. Richards, and . R. Cogan, Flight Test Evaluation of the SAFE-Cue System for Loss of Control Mitigation, In Proc. of AIAA Guidance, Navigation, and Control Conference, National Harbor, MD, January 2014.

[5]V. Stepanyan, K. Krishnakumar, J. Barlow and H. Bjil, Adaptive Estimation Based Loss of Control Detection and Mitigation, In Proc. of AIAA Guidance, Navigation, and Control Conference, Portland, Oregon, August 2011.

[6]J. Barlow, V. Stepanyan, and K. Krishnakumar, Estimating Loss-of-Control: a Data-Based Predictive Control Approach, AIAA Guidance, Navigation, and Control Conference, Portland, Oregon, August 2011.

[7]K. Krishnakumar, V. Stepanyan, and J. Barlow, Piloting on the Edge Approaches to Flight Control Solutions, In Proceedings of IEEE Fourth International Conference on Space Mission Challenges for Information Technology, Palo Alto, CA, August 2011.

[8]R. M. Hueschen, Development of the Transport Class Model (TCM) Aircraft Simulation From a Sub-Scale Generic Transport Model (GTM) Simulation, NASA/TM 2011-217169, August 2011.

[9]T.L. Jordan and W.M. Langford, Development of a Dynamically Scaled Generic Transport Model Testbed for Flight Research Experiments, In Proc. AUVSI Unmanned Systems North America, Arlington, VA, 2004.

[10]A.M. Murch and J.V. Foster, Recent NASA Research on Aerodynamic Modeling of Post-Stall and Spin Dynamics of Large Transport Airplanes, In Proc. 45th AIAA Aerospace Sciences Meeting and Exhibit, Reno, NV, 2007.

[11]J. Totah, K. Krishnakumar, and S. Vikien, Integrated Resilient Aircraft Control - Stability, Maneuverability, and Safe Landing in the Presence of Adverse Conditions, NASA Aeronautics Research Mission Directorate Aviation Safety Program, April 13 2007.

[12]N. Nguyen, K. Krishnakumar, J. Kaneshige, and P. Nespeca, Flight Dynamics and Hybrid Adaptive Control of Damaged Aircraft, AIAA Journal of Guidance, Control, and Dynamics, 31(3):751–764, 2008.